Lead zirconate titanate aerogel piezoelectric composite designed with biomimetic shell structure for underwater acoustic transducers

Xin Long,[ab] Xiongbang Wei,[b] Yuhong Qiu,[ab] Ming Jiang,[b] Zhi Chen,[ab] Yaocheng Song,[ab] Linnan Bi,[ab] Jianming Wang,[c] Sizhe Wang*[b] and Jiaxuan Liao*[ab]

[a] *School of Materials and Energy, University of Electronic Science and Technology of China, Chengdu 611731, China. Email: jxliao@uestc.edu.cn*

[b] *The Yangtze Delta Region Institute (Quzhou), University of Electronic Science and Technology of China, Quzhou, Zhejiang 324000, China*

[c] *Chengdu Aerospace Communication Device Company Limited, Chengdu, 610052, China*

PART1: Experimental process

Firstly, we successfully prepared PZT aerogels through solvothermal assisted sol-gel method and supercritical CO_2 drying method. After they were naturally annealed at 800℃ and sintered by hot pressing at 800℃, respectively, the crystallized PZT aerogels and PZT aerogel sintered sheets were obtained. Subsequently, the crystallized PZT aerogels were milled into powders and then combined with PVDF to form the PZT aerogel/PVDF composite coating by using 0-3 composite method. The surface of the obtained single-layer composite coatings was irradiated by high-power laser for a certain period of time, then they were rolled to obtain the 5-layer PZT aerogel/PVDF composite coating. Finally, by using the PZT aerogel/PVDF slurry as the coupling agent, 6 groups of 5-layer composite coatings and 5 groups of sintered sheets were alternately connected layer by layer to obtain the alternate coatings/sheets structure designed PZT aerogel piezoelectric composite, and its detailed size is about 20.0mm×20.0mm×2.6mm.

PART2: Experimental design ideas

1. The purpose of preparing PZT aerogel/PVDF composite coatings using PZT aerogels:

As the components of the PZT aerogel/PVDF composite coatings, the crystallized PZT aerogels still have a nanoporous structure and the change of the shape does not

affect their nanostructure, and the average particle size of the PVDF powders we purchased is about tens of microns. Thus, during the slurry preparation process, PVDF powders cannot enter the inner space of the crystallized PZT aerogel powders. Until the coatings are formed, the nanoporous structure of the crystallized PZT aerogel powders can still be maintained, which is the key to the low density of the composite coatings.

2. The purpose of preparing PZT aerogel sintered sheets using PZT aerogels:

In fact, our experimental scheme is based on overcoming the drawbacks in the preparation process of Pb-containing piezoelectric ceramics. Generally, Pb-containing piezoelectric ceramics are prepared by the oxide mechanical mixing method. The powder raw materials have coarse particles, and the particle size and purity cannot be guaranteed, resulting in extremely low activity, which leads to serious lead loss in the embryo body formed after molding powders during high-temperature sintering. Consequently, the resulting Pb-containing piezoelectric ceramics have rough structure and poor chemical uniformity, so that their piezoelectric properties cannot be effectively exerted.

The use of PZT aerogels to prepare PZT aerogel sintered sheets has the following advantages. Firstly, the PZT aerogels prepared by the solvothermal assisted sol-gel method have uniform structure, which provides a guarantee for the preparation of the PZT aerogel sintered sheets with uniform structure. Secondly, the newly-made PZT aerogels have a special pore structure with an average pore diameter of tens of nanometers, which effectively restricts the volatile Pb-containing compound molecules from leaving the aerogels at the beginning of sintering (similar to when used as a thermal insulation material, the nano-pore structure of aerogels inhibits the movement and collision of air molecules and weakens the convective heat transfer of air). During the sintering process, the gradual densification of the whole material under the hot pressing and the gradual disappearance of the pores make the interior always maintain a high vapor pressure of Pb-containing compounds, which inhibits the further volatilization of these compounds that are not volatile. Therefore, until the sintering is completed, most of the volatile Pb-containing compounds are not lost, and the uniform chemical composition of the PZT aerogel sintered sheets is also guaranteed. Finally,

the density of PZT aerogels is very low, and the density of the PZT aerogel sintered sheets can be controlled by only controlling the time when sintering above the crystallization temperature. Based on the above reasons, we selected PZT aerogels as raw materials to prepare PZT aerogel sintered sheets.

PART3: The application properties' comparison of the PZT aerogel piezoelectric composite and 5 kinds of Pb-containing piezoelectric ceramics and one kind of non-leaded piezoelectric ceramic $BaTiO_3$ in UATs

Detailedly, UATs' signal transmission and driving ability depends on the hydrostatic piezoelectric coefficient d_h of piezoelectric materials (Eq. S3), signal receiving sensitivity depends on the hydrostatic pressure voltage coefficient g_h of piezoelectric materials (Eq. S4), electrical comprehensive properties depends on the hydrostatic pressure figure of merit *HFOM* of piezoelectric materials (Eq. S5), power loss depends on the dielectric loss $tan\delta$ of piezoelectric materials, acoustic-electric signal conversion capability depends on the planar electromechanical coupling coefficient k_p of piezoelectric materials, and signal transmission degree depends on the acoustic impedance Z matching of piezoelectric materials and water, which mainly depends on the density ρ of piezoelectric materials (Eq. S1). In order to verify and evaluate the properties' improvement ability of the PZT aerogel piezoelectric composite on UATs, we used 5 groups of Pb-containing piezoelectric ceramics and 1 group of non-leaded piezoelectric ceramics $BaTiO_3$ with the same thickness as the control groups, and the comparison results are shown in Fig. S9. It can be known that the PZT aerogel piezoelectric composite achieves higher hydrostatic pressure piezoelectric coefficient d_h, higher hydrostatic pressure voltage coefficient g_h, higher hydrostatic pressure figure of merit *HFOM*, *lower* dielectric loss $tan\delta$ at 40Hz and lower density ρ. Also, it also achieves the planar electromechanical coupling coefficient k_p higher than that of the non-leaded piezoelectric ceramic $BaTiO_3$ and similar to that of Pb-containing piezoelectric ceramics. Meanwhile, as already analyzed before, the PZT aerogel piezoelectric composite prepared based on the design principle of the biomimetic shell structure has natural comprehensive mechanical properties'

advantages due to its role as an energy dissipation mechanism in the stress field and as a defect-resistant material, thus it has good practical significance and use value in UATs.

$$T=\frac{2Z_{pie}}{(Z_{wat}+Z_{pie})^2} \quad \text{(S1)}$$

Where T is the signal transmission degree of UATs; Z_{wat} and Z_{pie} are the acoustic impedance of water and piezoelectric materials, respectively. $Z=\rho C$, ρ is the density of propagation media of sound waves; C is the propagation speed of sound waves in propagation media.

$$k_p^2=(f_p^2-f_s^2)/f_p^2 \quad \text{(S2)}$$

Where k_p is the planar electromechanical coupling coefficient; f_p is the anti-resonant frequency; f_s is the resonant frequency.

$$d_h=d_{33}+2d_{31} \quad \text{(S3)}$$

$$g_h=d_h/\varepsilon_0\varepsilon_r \quad \text{(S4)}$$

$$HFOM=d_h \times g_h \quad \text{(S5)}$$

Where d_h is the hydrostatic pressure piezoelectric coefficient; d_{33} and d_{31} are the piezoelectric coefficients with different orientations, d_{33} and d_{31} of PZT piezoelectric materials have opposite signs; g_h is the hydrostatic pressure voltage coefficient; ε_0 is vacuum permittivity, which is equal to $8.854187817\times10^{-12}$ F/m; ε_r is the relative permittivity.

PART4: The fatigue test of piezoelectric properties of the PZT aerogel piezoelectric composite

In this test, we used the ZJ type piezoelectric coefficient tester to continuously apply the pressure of the alternating frequency 110Hz and the magnitude of 1.2N to the prepared PZT aerogel piezoelectric composite to judge its anti-fatigue ability through the change trend of its piezoelectric coefficients d_{33} and d_{31} over time. The total test time is 7 days, and data is recorded every 12h on average. The test results obtained are shown in Table S2. It can be seen that the piezoelectric coefficients d_{33} and d_{31} of the

PZT aerogel piezoelectric composite did not change significantly during the 7-day test, indicating that the composite has good anti-fatigue ability, which provides a guarantee for its application in the actual environment.

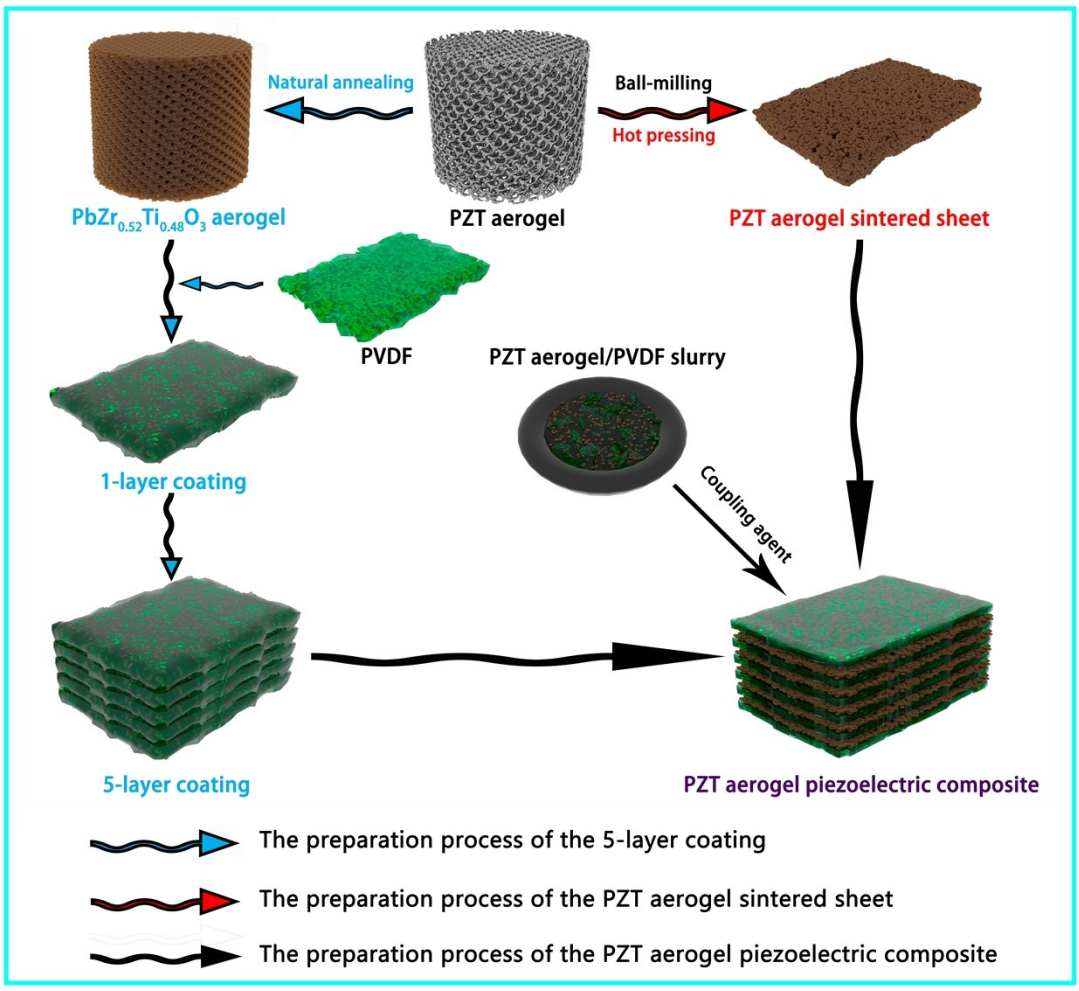

Fig. S1 Schematic illustration of the synthesis process of the PZT aerogel piezoelectric composite.

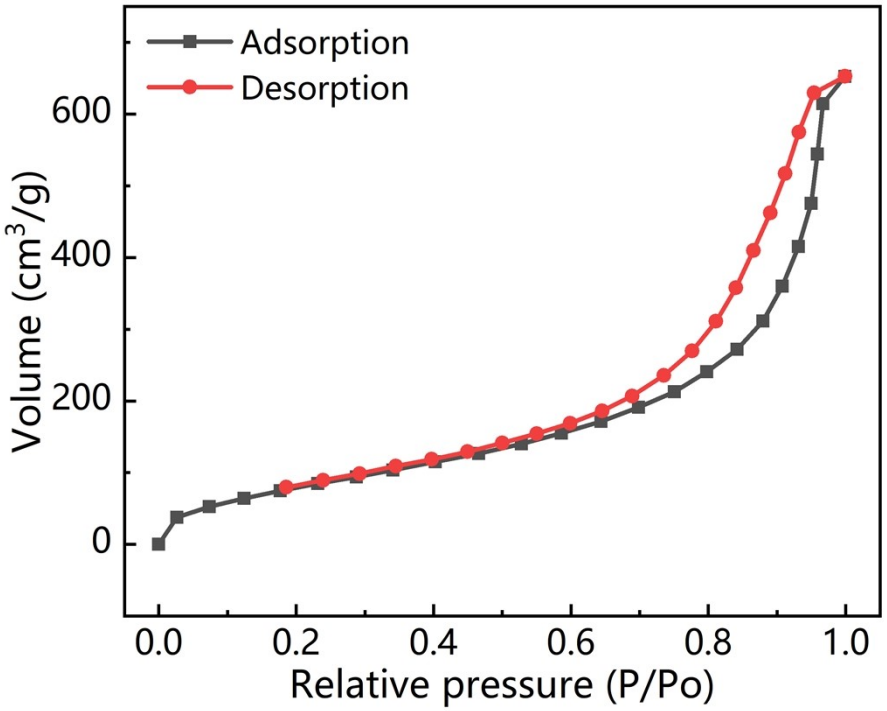

Fig. S2 N_2 adsorption and desorption isotherm of the freshly made PZT aerogel.

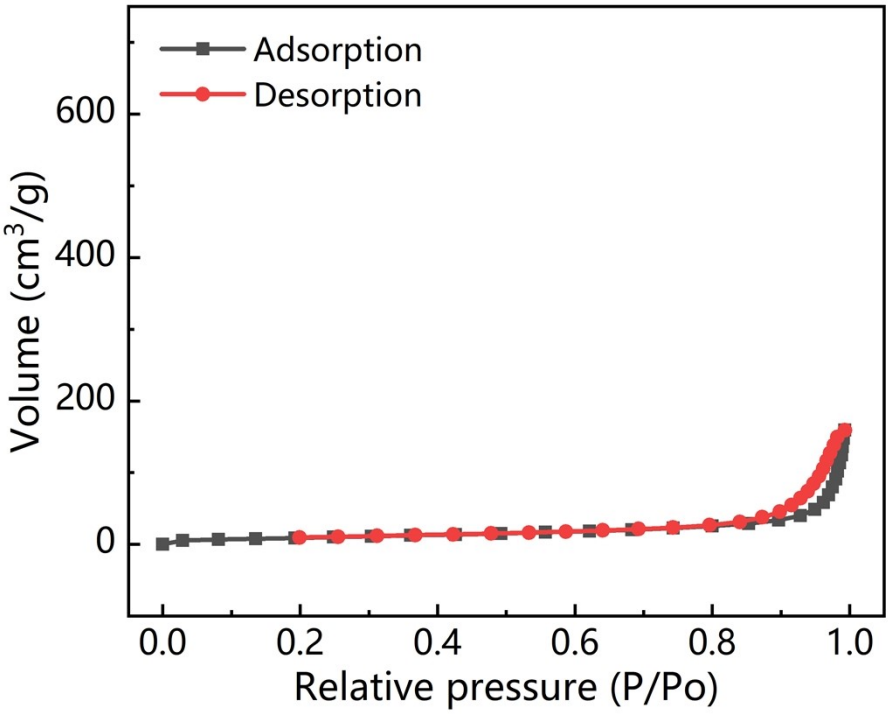

Fig. S3 N_2 adsorption and desorption isotherm of the PZT aerogel treated by natural

annealing at 800℃.

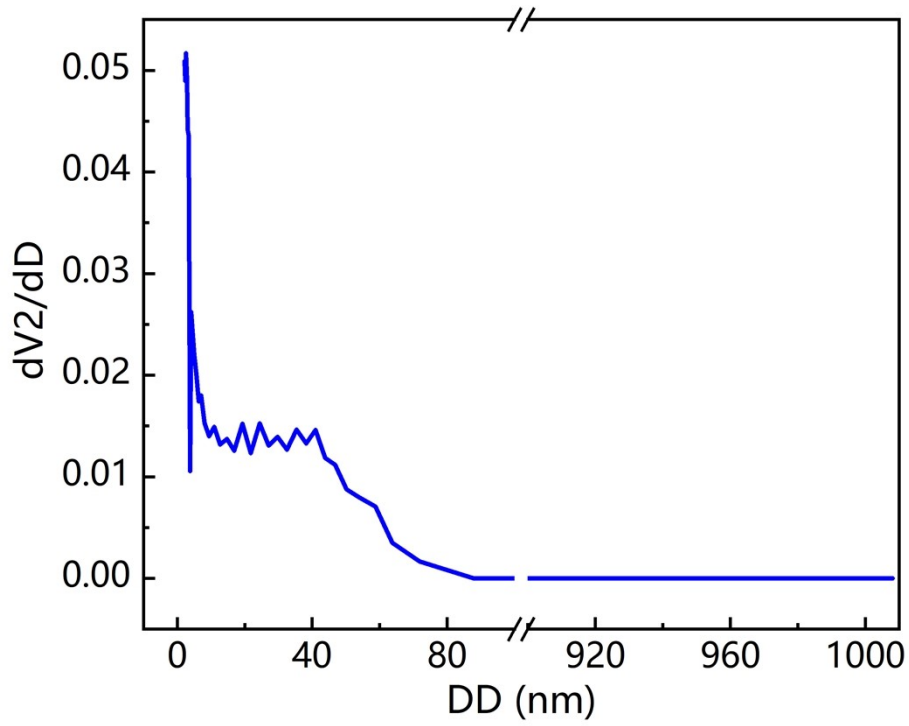

Fig. S4 Pore volume-pore size distribution curve of the freshly made PZT aerogel.

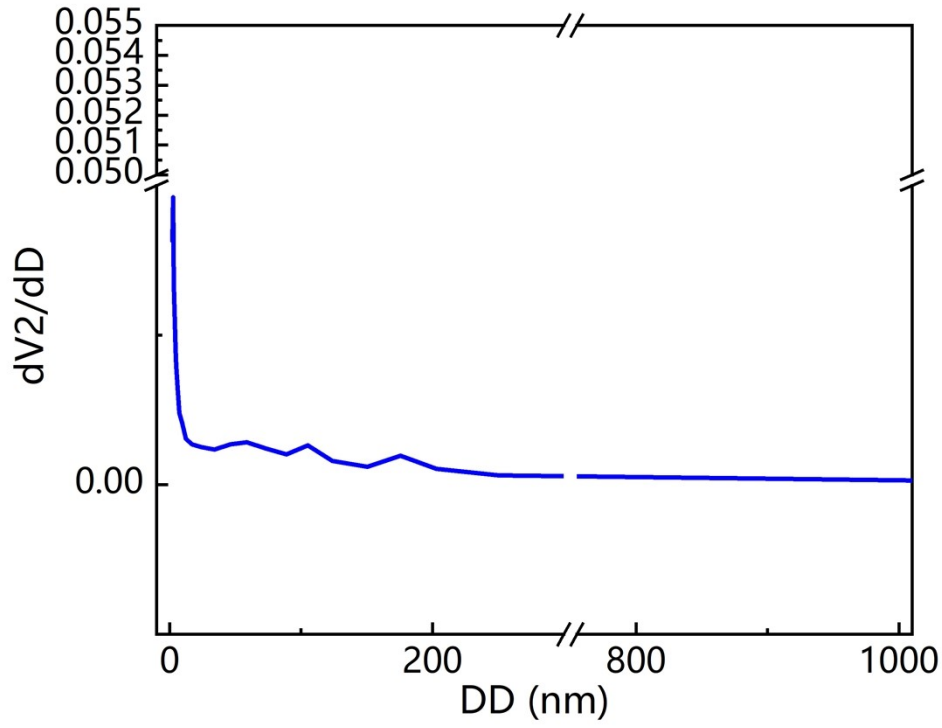

Fig. S5 Pore volume-pore size distribution curve of the PZT aerogel treated by natural annealing at 800℃.

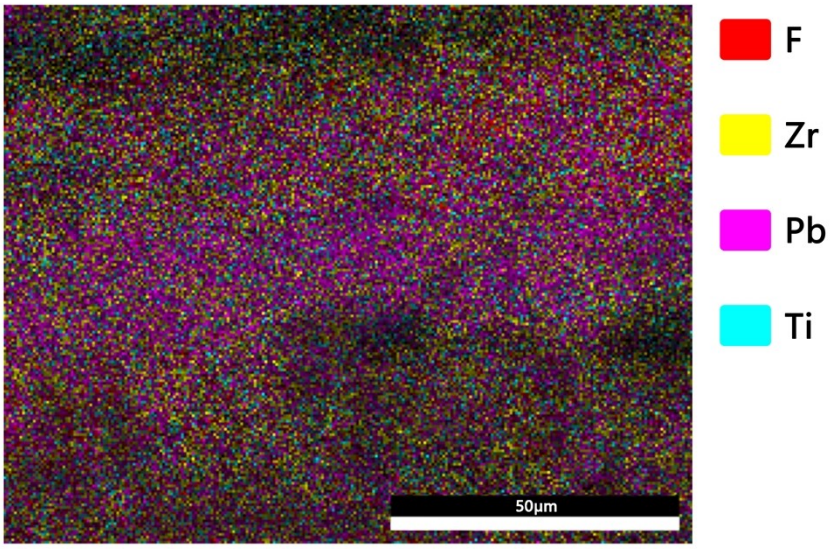

Fig. S6 The EDS image of longitudinal cross-section of the 5-layer PZT aerogel/PVDF composite coating.

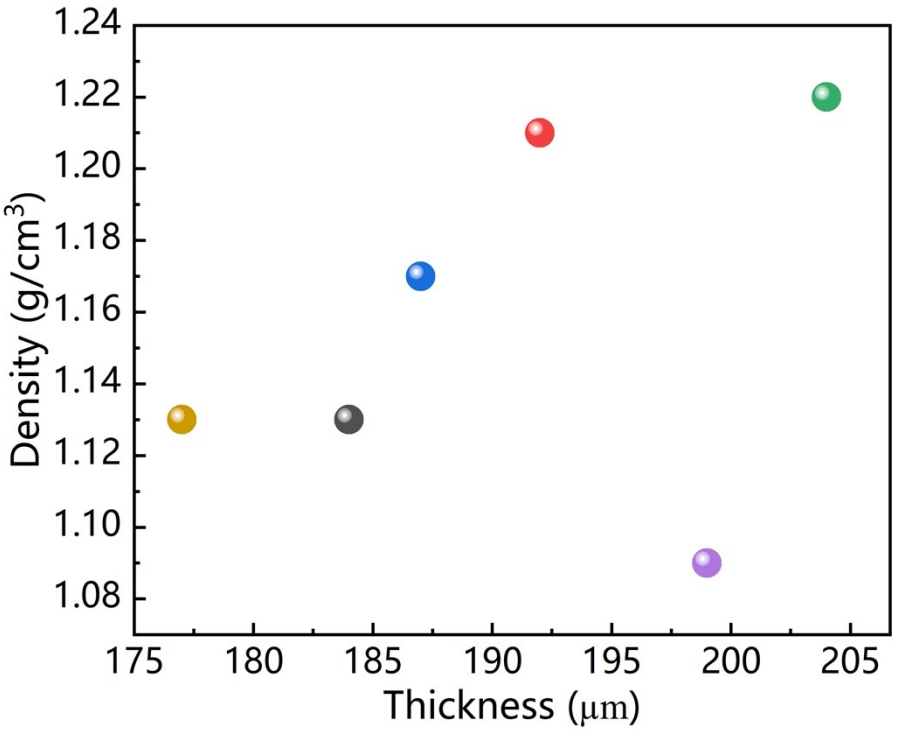

Fig. S7 The thickness and density of the PZT aerogel composite coatings constituting the PZT aerogel piezoelectric composite.

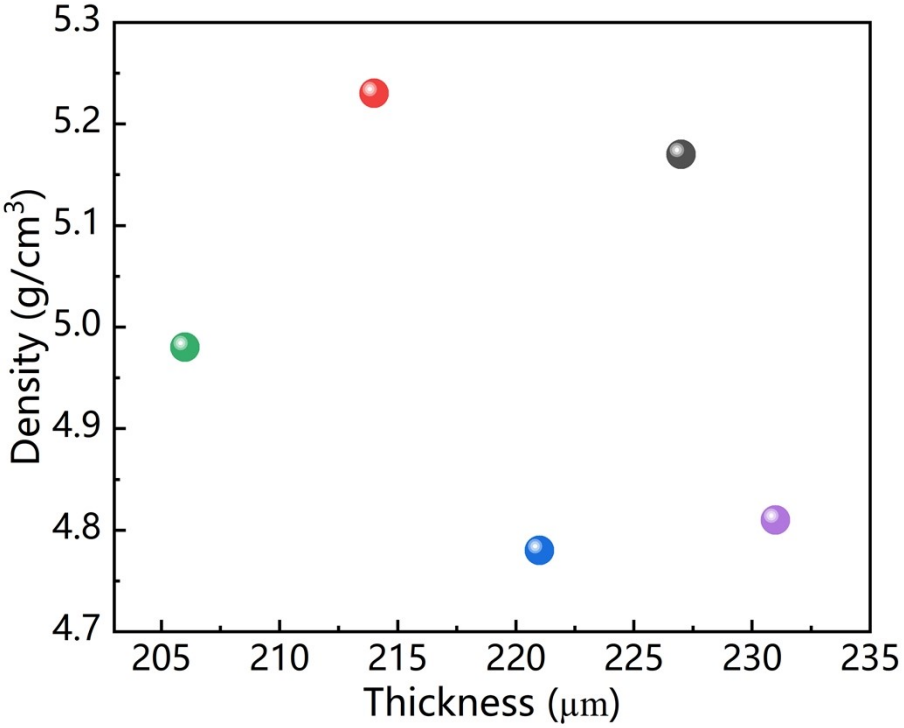

Fig. S8 The thickness and density of the PZT aerogel sintered sheets constituting the PZT aerogel piezoelectric composite.

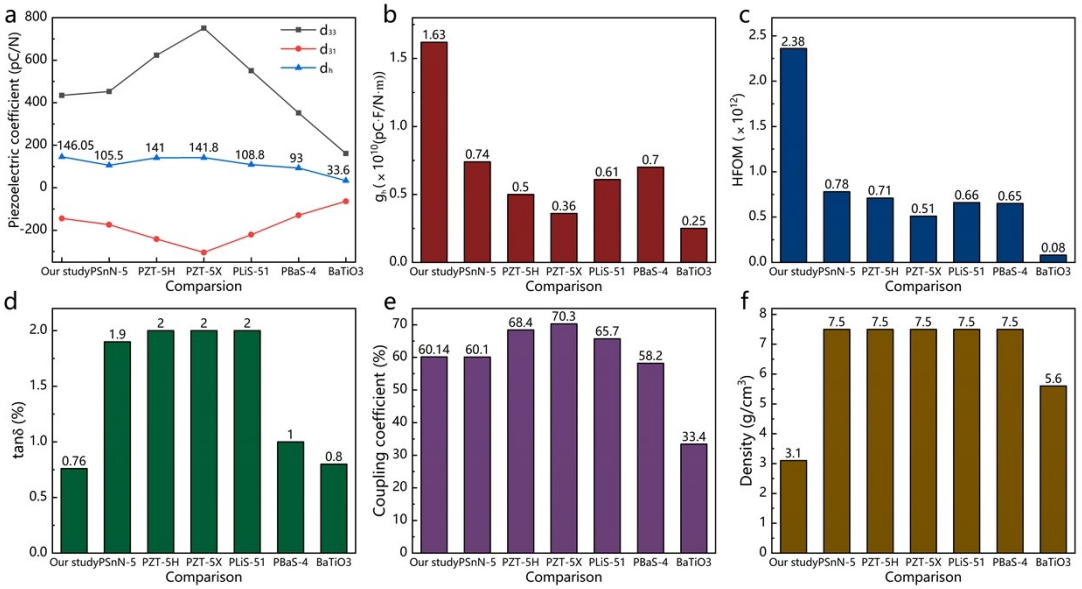

Fig. S9 Comprehensive properties' comparison of the PZT aerogel piezoelectric composite and control groups in UATs. (a) hydrostatic piezoelectric coefficient d_h; (b) hydrostatic pressure voltage coefficient g_h; (c) hydrostatic pressure figure of merit *HFOM*; (d) dielectric loss *tanδ*; (e) planar electromechanical coupling coefficient k_p; (f) density ρ.

Table S1 Test results of piezoelectric coefficients d_{33} and d_{31} of the PZT aerogel piezoelectric composite

TIME	**1**	**2**	**3**	**4**	**5**	**6**	**7**	**8**	**9**	**10**
D_{33}(PC/N)	434.2	431.8	438.6	437.7	435.8	437.5	432.9	434.8	435.6	432.6
D_{31}(PC/N)	-144.3	-144.2	-142.9	-145.6	-143.7	-144.3	-146.1	-145.0	-144.8	-144.6

Table S2 Test values of piezoelectric coefficients d_{33} and d_{31} of the PZT aerogel piezoelectric composites at different time nodes

TIME(H)	**0**	**12**	**24**	**36**	**48**	**60**	**72**	**84**	**96**	**108**
D_{33}(PC/N)	435.1	435.1	435.0	435.2	435.1	435.1	435.0	435.1	435.0	435.0
D_{31}(PC/N)	-143.9	-144.0	-144.0	-144.0	-144.1	-144.0	-144.1	-144.1	-144.1	-143.9
TIME(H)	120	132	144	156	168					
D_{33}(PC/N)	435.0	435.1	435.2	435.1	435.0					
D_{31}(PC/N)	-144.0	-144.0	-144.0	-144.1	-144.0					